MSc in Photonics

PHOTONICS**BCN**

Universitat Politècnica de Catalunya (UPC)
Universitat Autònoma de Barcelona (UAB)
Universitat de Barcelona (UB)
Institut de Ciències Fotòniques (ICFO)

http://www.photonicsbcn.eu

Master in Photonics

MASTER THESIS WORK

Precision of cavity-enhanced optical rotation measurements

Joaquín Guimbao Gaspar

Supervised by Dr./Prof. Morgan.W.Mitchell, ICFO

Presented on date 22th July 2016

Registered at

Escola Tècnica Superior d'Enginyeria de Telecomunicació de Barcelona

Precision of cavity-enhanced optical rotation measurements

Joaquín Guimbao Gaspar

Quantum information with cold atoms, Morgan Mitchell group at the Institute of Photonic Sciences (Barcelona, Spain)

joaquinguimbao@gmail.com

Abstract: The signal to noise ratio in atomic magnetometry is fundamentally limited by the optical depth of the atomic ensemble. During the last decade, different technics for optical depth enhancement has been developed by several groups, some of them involving the implementation of an optical cavity. This thesis evaluates the performance of such an implementation by the polarization read out noise analysis of an optical cavity with similar characteristics as the already implemented by other groups. We obtained an estimated value for the signal to noise ratio enhancement with a cavity of 171 Finesse, and we studied the behaviour of the different sources of polarization noise in this system.

Keywords: Atomic magnetometry, Cavity enhancement Faraday rotation, Cavity enhancement spin squeezing

1.Introduction:

This thesis was developed at the Morgan Mitchell group of Quantum Information with cold atoms, at ICFO. Through the generation of particle entanglement in form of a squeezed spin state in an atomic cloud of 87Rb atoms, via Quantum Non demolition Measurements, their current quantum limited atomic magnetometer is able to measure magnetic fields over several millimetres with a resolution of micrometres, and sensitivities down to the order of pT/$\sqrt{Hz}$. They achieve a quantum noise reduction by 3dB, and metrological sensitivity is improved by 2dB beyond the standard quantum limit of a coherent spin state [3].

A schematic picture of the basics of their experiment set-up is normally introduced by the following way:

Figure 1: Schematic of the Atomic magnetometer set-up [6].

The Probe input beam projected in S_x polarization, experiment a Faraday rotation after crossing the atomic ensemble, through an homogeneous coupling with the collective pseudospin degree of freedom **F** of the atomic cloud. This rotation tilt ∅, relates with F_z by the following expression [4]:

$$\emptyset = gF_z \quad ; \quad g = \frac{\sigma_0}{A} \cdot \left(\frac{\Gamma}{\Delta}\right) \tag{1}$$

Where g is the coupling constant from the interaction Hamiltonian of the coupling between atom spins and light polarization observables[1], σ_0 the resonant cross section , A the cross sectional area, Γ the linewidth of the atomic state, and Δ the detuning . At the output we measure the rotation angle ∅ with a shot noise limited balanced polarimeter. The variance of the outcome ∅ is given by:

$$var(\emptyset) = g^2 var(F_z) + V_{RO} \quad (2)$$

V_{RO} is the readout noise from the measurement, which basically involves the electronic noise from the detector electronics, quantum noise (shot noise) from measuring the optical polarisation, and technical noise introduced into the polarization. Technical noise may come from various sources, such as intensity or frequency noise of the laser, or mechanical instabilities from the optical elements. As a signal to noise, we can take the ratio between the two terms in equation (2), and since for an input coherent spin state $var(F_z) = \frac{N_A}{2}$ (N_A number of atoms):

$$SNR = \frac{g.\frac{N_A}{2}}{V_{RO}} \quad (3)$$

With SNR$\cdot \frac{2}{N_A}$ the signal to noise ratio for a single atom. In their current experiment they achieve a SNR$\sim$1 loading around 500 atoms; having a g$\sim 10^{-7} rad/atom$.

The fundamental limitation for the SNR is related with the effective resonant optical depth "OD_0" of the atomic ensemble:

$$SNR^2 = OD_0 \cdot \gamma \quad ; \quad OD_0 \sim = \frac{\sigma_0}{A} N_A \quad ; \qquad SNR = g^2 N_A N_L \quad (4)$$

Where $\gamma = \frac{\sigma_0}{A} (\frac{\Gamma}{\Delta})^2 N_L$ is the fraction of atoms that scatter a photon, and A effective interaction cross section between light and atomic ensemble, and N_L number of photons. Increasing the optical depth, imply a reduction of the cross sectional area. On the other hand, reduction of cross section area brings an inhomogeneous coupling with light along the atomic ensemble. This latter effect introduces then a limit in the performance of our apparatus, which at this time achieve the mentioned resolution for a found optimal value of the optical depth about $OD_0 \sim 50 - 100$.

Over the last 10 years, different strategies for increasing the effective optical depth avoiding this issues, has been proposed. One of them, elaborated by Ian Daniel Leroux at the MIT (2011) and Monika Hellen Schleier-Smith also at MIT (2011), involves the use of an optical cavity.

To understand the benefits of such an implementation, recall first that our light-induced squeezing methods rely on probing the collective spin variable F_z of the ensemble. Knowing this quantity beyond the standard quantum limit, imply either knowing the states of the individual atoms, or he anti-correlations between them. Revealing individual states collapses the superposition, and reduce the signal $|\langle F_x \rangle|$, so we are only interested in the latter, obtaining collective information avoiding revealing individual states [2]. This can only be achieved by ensuring that the dominant scattering process is collective scattering into a single mode (forward scattering into the cavity mode). Detrimental free-space scattering (non-forward-scattering in to the cavity mode), reveal the individual states causing decoherence and introducing spin noise. This is a fundamental limitation to light-induced squeezing, which depends on the ratio of photons scattered into the cavity, and photons scattered into free space: the cooperativity "γ", our figure of merit in the cavity enhanced atomic magnetometer [1]. The enhancement of the g constant by the atomic cooperativity can be expressed as:

$$g_{cav} = \frac{2\mathcal{F}}{\pi} g \quad (5)$$

Where $\mathcal{F}$ is the Finesse of the cavity. Effective Optical depths enhanced by this cooperativity can reach values about $OD_0 \sim 10^4$. In this conditions, previously mentioned MIT projects has achieved metrological squeezing about 1.5dB, and Allan variance decrements of 2.3.

Despite the evident benefits of such an implementation in the amount of signal of the outcome of our experiment, the implementation of any optical device able to have impact in the polarization state of the probe beam, will have consequences in the signal to noise ratio of our outcomes.

The challenge of this thesis is to determine if such an implementation would have net benefits in the signal to noise ratio of the outcome in our current set-up. This was achieved by measuring the polarization technical noise introduced by a spherical symmetric Fabry-Perot cavity with Finesse 1000, into the probe beam. By comparing the noise added by the cavity, with the expected theoretical increase of the enhanced signal, we can in principle determine if the implementation of this cavity in our set-up will bring or not an improvement in the signal to noise ratio.

With this purpose, the project involved the following main aims: (1) Calculations for the design of the cavity. (2) Build up the cavity. (3) Characterize the cavity. (4) Lock the laser to the cavity. (5) Polarization read-out noise measurement with balance detection. (6) Measurement of the birefringence of the cavity. We first used a "test cavity" already built in the lab, for learning about the characterization procedure, and after we built up our own cavity for the mentioned measurements.

2. Results:

2.1 "Test cavity" characterization:

We scanned the frequency of the emission of our Toptica DL100 ECDL over a range of 3.8GHz at a frequency of 100 kHz. This range allowed us to observe the whole free spectral range. Also for this frequency the peaks had a reasonable good fit to a Lorentzian.

We used a saturated absorption spectroscopy signal, as an atomic reference for the frequency calibration of the transmission signal from the cavity. Triggering both cavity transmission and spectroscopy signals with the scanning of the Toptica we obtained the following traces for cavity transmission:

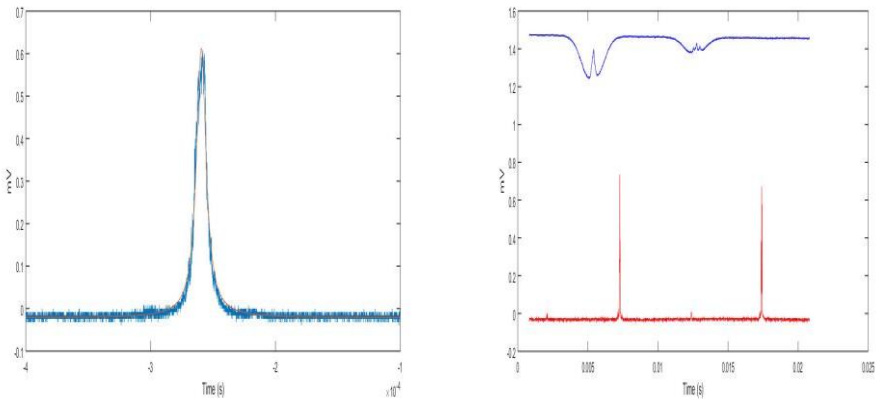

Figure 4: (a) Transmission (23%) Peak zoomed. (b) Transmission peaks over a FSR

Figure (4b) Shows cavity transmission peaks corresponding to the excitation of the TEMoo modes sequence over one free spectral range, with y-axis in arbitrary units. Figure (4a) show the zooming of a single peak. We used two hyperfine components of the 87Rb D1 line: F=1 -> F=1; and F=2->F=1, for the calibration of the x-axis in frequency units. For the estimation of the width of the peak, we performed a Lorentzian fit of the experimental points, and we took the FWHM value.

Free spectral range ω_{FSR}, Finesse F, and Quality Factor Q of the cavity, can be obtained by:

$$\omega_{FSR} = \frac{c}{2L} \quad ; \quad F = \frac{\omega_{FSR}}{\Delta\omega} \quad ; \quad Q = \frac{\omega}{\Delta\omega} \tag{6}$$

Where L is the separation between mirrors and c the speed of propagation of light inside the cavity. From here we could estimate the results for the characterization parameters, which are presented in the following table:

Finesse	171
Free Spectral Range (GHz)	2.4
Linewidth (MHz)	14
Distance L (cm)	6.2
Beam waist (μm)	87

Table 1: Test cavity parameters

2.2 Laser-Cavity Lock in:

We filtered the cavity reflection signal with a 1KHz low pass filter in order to remove some acoustic noise coming from vibrations of the mirrors, and we mixed it with the local oscillator signal in the Pound Drever Hall detector unit from our Toptica. We found the optimal value for the relative phase between this two signals tuning the phase shifter to the right position. At this configuration, the error signal proportionated by the PDH detector was the following:

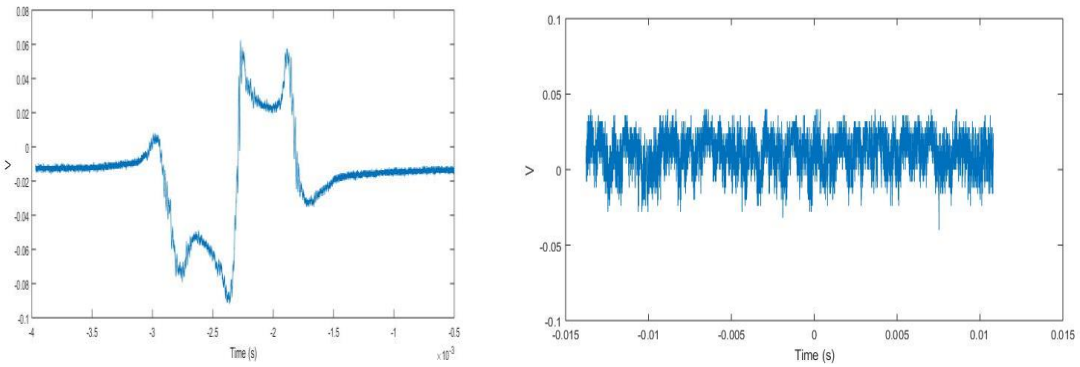

Figure 5: (a) Error signal from the Pound Drever Hall. (b) Error signal with lock in.

We found the right PID values in the PID regulator unit from our Toptica, for having an optimal lock in signal, following the next procedure: 1: Set P,I and D gains to 0. 2: Start adding P gain until you are able to see oscillations. 3: Reduce that value to the half, and start adding I gain until you see oscillations again. We didn´t had to concern about the differential gain in order to obtain a reasonable good lock in signal. We used as a metric of the quality of the signal the ratio of the rms value: 15 mV, of the error signal once we activate the lock (Figure 2), and the size of the error signal: 200 mV (Figure 1).

3.3 Balanced detector characterization:

Gain (G): By sending light to just one of the two photodiodes, we measured the output voltage signal of the detector against the input optical power in order to calculate the overall gain of the internal circuit plus the photodiodes. We obtained a value of $7.036 \cdot 10^6$ V/W, which is on the order of magnitude we expected.

Bandwidth: Analysing the signal from the detector in frequency domain with the spectrum analyser, we estimated form our measurements a cut-off frequency at 200KHz.

Noise: Now here we report the noise analysis of the detector without the cavity contribution. In a linear detection system, noise power N on the electronic output will depend on the optical input power P as:

$$N = C + BP + AP^2 \quad [5] \qquad (7)$$

Where the terms C represent the electronic noise from the electronics of the detection, BP the Shot Noise, and AP^2 the technical noise contribution. Determining this noise scaling with input power we can establish the dominating noise contribution in each range of input optical powers. Particularly, in the region where the linear term dominates: $B/C < P < A/B$, we say that the detector is shot noise limited (SNL), meaning that the mean source of noise arises in quantum fluctuations of the system. Range with technical noise the dominant term, noise contributions from polarization imbalance of the detector, or mechanical instability of the optical elements, are the most important.

Again with the Spectrum Analyser we collected the noise spectral density at each frequency, for input powers from 0.3 μW to 3209 μW. We scanned over a range of frequencies inside the bandwidth of the detector (0 Hz to 200KHz), with a resolution bandwidth of 300 Hz and a video bandwidth of 3 KHz:

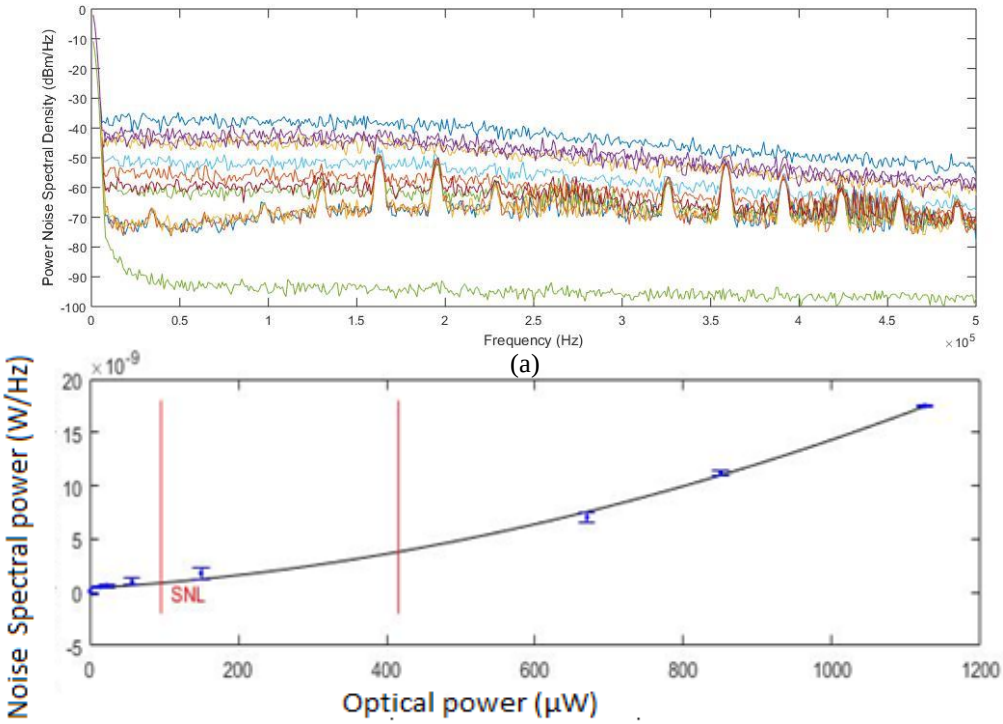

Figure 6: (a) Power Noise Spectral Density of the signal from the detector. The one on the bottom corresponds to the noise of the spectrum analyser, The second one on the bottom is the electronic noise of the detector.The rest of the plots corresponds to the nosie coming from thedifferent optical powers input signals. (b) Power Noise against optical input power for 300KHz frequency. Red lines corresponds to the limits (C/B),(B/A) of

Here the power noise spectral density is given in dBm/Hz. You can convert this quantity in to Watts/Hz through the transformation:

$$P = 10^{\frac{P_{dBm}}{10}}/1000 \tag{8}$$

And obtaining the total power just multiplying this quantity by the bandwidth of the detector. For a given frequency of 300KHz, we fitted the polynomial of equation (7), (first converting from log scale in to linear scale using (8)) in order to determine the extension of the shot noise limited range (Figure 6b):

Electronic noise C (W)	3.958e-10 ± 1.22 e-11
Shot Noise B (W)	4.11e-12 ± 4.2e-13
Technical noise A(W)	9.8141-15± 5.2e-16

Table 2: Characterization of the detector

We can clearly identify in figure (6b) the three different regions where each of the contributions is dominant. By the fitting parameter we could determine that the SNL range of the detector at the frequency of 300KHz is confined around [96 μW, 419.97 μW].

2.3 Technical Noise added by cavity:

In this section we will again analyse the noise in the detection system but this time with the cavity contribution. We don´t expect to observe in principle differences in electrical noise ground level and linear scaling in SNL region, since we maintain the same configuration of all elements in our set-up. The PNSD curves from powers going from 0.3 W to 500 W are showed below:

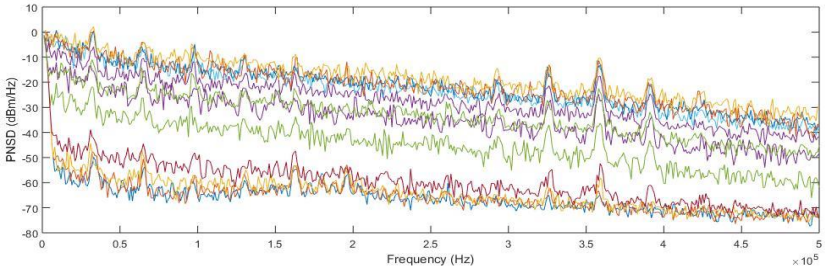

(a)

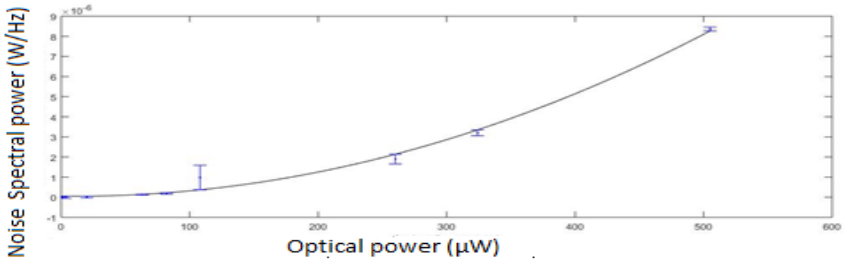

(b)

Figure 7: Power Noise Spectral Density of the signal from the detector, and Power noise for 300KHz against optical power.

By the same procedure as in the previous subsections, in order to perform the fit we have to first convert dBm in to W, and pick up a frequency to analyse the polynomial noise behaviour. The results are quite different in this case: We used equation (7) with B and C fixed to the values without the cavity, and fitted to find A_{cav}.=2.197e-11± 4.1e-11, fits the curve. This means that the addition of the cavity increases technical noise in such a way that noise dependence with the input power is mostly quadratic, and there is not shot noise limited range.

Most important source of technical noise in this measurement was the bad quality of the error signal for the lock in of the laser to the cavity. For cavity locks with relatively high finesse, a good mechanical stability of the system is required. A high finesse cavity, with pretty narrow transmission peaks, and with not particularly good stability, leads to an extremely noisy error signal, since vibrations change constantly the shape and position of the peak. A high rms value in the error signal once the laser is locked, translates directly to high intensity fluctuations at the output of the cavity, which in our case, contribute with a great impact in the technical noise of the in-put light in the detection.

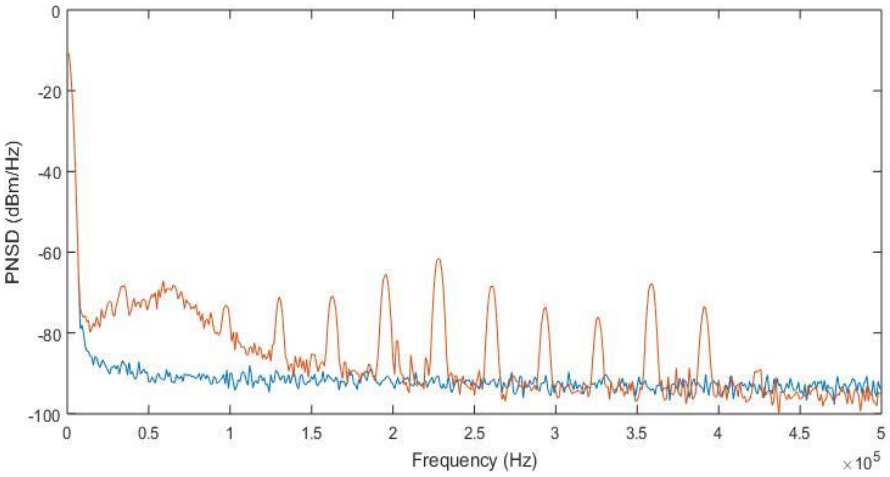

Figure 8: Blue trace corresponds to the noise of the laser without lock in. Orange trace is the noise once the laser is locked

In Figure (8), we can compare the spectral noise power from the laser with the noise introduced by the error signal. Data clearly confirm that the error signal we are using to lock is introducing probably the dominant contribution to the technical noise.

2.4 Figures of merit discussion:

We are now interested in calculating the resulting change in signal to noise ratio after implementing the cavity in our system. First we need to estimate the beam waist of the TEMoo Gaussian beam inside the cavity, in order to introduce this value in the cross section area A of equation (3). The beam waist *w* in a symmetric Fabry-Perot resonator relates with length between the mirrors by the following expression:

$$w = \sqrt{\frac{L\lambda}{2\pi}} \tag{8}$$

Which with the values measured in the characterization of our test cavity, gives a value of w=1.88e-4 m. We can estimate now from equation (1) the value of the g parameter, which give us g=8.3e-8 rad/atom.

Without the cavity, for a power of P= 280 μW , at frequency w=300KHz , the standard of the signal is 2.4e-9 W/Hz. To obtain the V_{RO} for this quantity we just have to convert this standard deviation of the signal in electronic Watts in the detector, to the optical power standard deviation. This is achieved by converting first from electronic W to V. (just multiplying by a 50 ohms resistance and taking the square root) and multiplying by the gain of the detector G. So for this case V_{RO}= 3.4e-16 W. We can now compute the signal to noise with (3), which gives SNR=33.2.

With the cavity, we have at that optical power and frequency, we have a value of V_{RO}=3.1e-13 W The value of g_{cav} using eq. (5) for this Finesse is g_{cav} = 9.04e-6rad/atom. Which leads to a SNR_{cav}=2.6. Which leads to a SNR_{CAV}/SNR=0.07.

3. Second cavity design:

We would like now to extract similar conclusions from a cavity with predefined parameters, whose TEMoo matches the spatial distribution of our atomic ensemble, and with bigger Finesse to increase the enhancement of the cooperativity g.

In our current set-up we have $g = 10^{-7}$ at $\Delta = 600$ MHz with $A = 3 \times 10^{-9}$ m^2. The atomic cloud has a gaussian width about 20um, and the probe beam has a beam waist matched to this width. Ideally our cavity would have the same beam waist. However, achieving this requires a confocal cavity with a radius of curvature (and separation between the mirrors) of about 0.5cm. This is too small – we cannot fit a MOT to make a cold atomic cloud inside this cavity. Instead, we follow the parameters of the Vuletic group, with a beam waist of ~50um.

The resonator implemented in our set-up, will be glued in a fixed position inside the vacuum chamber. Realignment of the mirrors won´t be possible once the cavity is set-up in place. For this reason, we are looking for a resonator as less sensible to misalignment as possible. Confocal Fabry Perot resonators have the minimum waist at the position of the mirrors. This minimize the angular divergence of the beam inside the resonator, which reduce the sensitivity to misalignment, and the effect of aberrations, making the confocal configuration the most stable.

On the other hand, we are interested in a homogeneous coupling between the beam and the atomic ensemble, so we need to excite exclusively the TEMoo mode of the resonator. In confocal configuration, transversal modes are degenerated in the same frequency, so once we lock the cavity, we will excite a superposition of all transversal modes instead of having a homogeneous Gaussian beam inside the cavity. To solve this compromise, we will work in a configuration as close to the confocality as possible, but far enough to distinguish between the TEM_{ml} family.

The TEMoo mode of the cavity, must match the spatial geometry of the atomic ensemble. With this aim. We choose two 2.5 cm radius of curvature mirrors of half inch, which gives a TEMoo mode of 57 micrometres of beam waist, and a Rayleigh range of 1.25 mm. To achieve confocal configuration, the distance between the mirrors must be then 2.5 cm.

The cavity parameters we expect for this configuration are:

Finesse	1000
Width (MHz)	6
Free Spectral range (GHz)	6
Beam waist (μm)	54
Expected g (rad/atom)	$0.636 \cdot 10^{-4}$

Table 3: Expected cavity parameters

3.1 Set-up:

Beam profiling: We first made calculations for the lenses of the telescope necessary to match the beam spatial characteristics of the TEMoo mode. We used GaussianBeam simulator to calculate this values. In order to have the most possible stable system, we also calculated the focal values which lead to a configuration with minimum sensibility to relative displacement between the lenses. After setting up the telescope we performed a beam profiling of our input beam with a CCD camera. We measured a 67 micrometers beam waist beam placed at 500mm from the telescope, meaning a 98% coincidence with the GaussianBeam simulator.

Alignment: We first set-up the cavity at 500mm from the telescope making sure that the reflected beam retraces the input beam. In this cavity configurations we have spherical symmetry, so the alignment procedure reduces to just find the centre of the spherical cavity, without taking special care to the angle of incidence. This was achieved by looking at the transmission detection: When the input beam doesn´t match the centre of the cavity, ray roundtrips are twice larger than when everything is well centred. This has a proportional impact in the free spectral range in transmission. So the task consists in finding the proper alignment to reduce the free spectral range to the half we have at the starting point.

Mode matching: Both absolute position of the telescope, and relative position between the lenses has an impact in the overlap between the input beam and the cavity TEMoo mode. Iteration between this two positions allows to find a maximum in transmission for the Gaussian mode. Once this is achieved, reflected beam must be collimated after passing back through the telescope.

3.2 Characterization:

Following a similar procedure as in previous sections we obtained the traces of the transmission peaks over several free spectral ranges with the atomic reference:

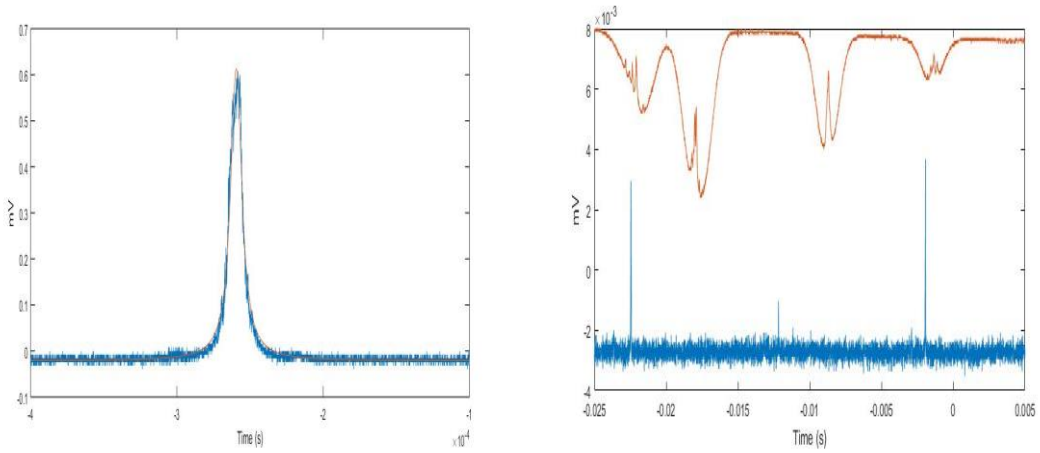

(a) (b)

Figure 8: (a) Transmission Peak zoomed. (b) Transmission (19%) peaks over a FSR

Finesse	413
Width (MHz)	15
Free Spectral range (GHz)	6.2

Table 4: Cavity Characterization

A difference in intensity between the two peaks can clearly be observed. This is because for this cavity, to be able to scan over the whole free spectral range, we had to open the scan much more than for the previous cavity. Several processes that can lead to changes in the output power of the laser can take place during the expansion of the piezo during the scanning (the laser cavity changes its length, the current implemented to the diode is self-correcting, etc…). So this difference can be explained in terms of different in put lights intensities arriving to the cavity at two different points of the scan.

Another important appreciation is that, despite we achieved a good mode matching and alignment, the transmission is quite low. As already have been mentioned in the previous sections, due to the spherical symmetry of the problem, the set-up of a symmetric spherical confocal Fabry Perot cavity relies in just two main issues: The mode matching, and finding the centre of the cavity. From Figure 1, it´s clear that centre of the cavity has been found successfully, since no other modes appears at different frequencies, and the free spectral range is inversely proportional to twice the length of the cavity. We performed a beam profiling of our input beam, and we observed that it matches the theoretical TEMoo of the cavity with a 97% of overlap, so the mode matching wasn´t the problem neither. The time of integration of our detection system is about 1 ns, so since the expected cavity width is about 6MHz, there is not possibility that we are filtering the

transmission signal. It neither has to do with the frequency of our scanning, since we observed that changing this variable didn´t had any effect on the transmission signal.

The only factor that could explain such a decrement of the transmission signal are diffraction losses. Could be that mirrors wasn´t clean enough, or that could be some important aberrations in their surfaces.

The system presented a huge mechanical instability. As a consequence the, the error signal coming from the PDH detector was too noisy. The combination between the fact that this transmission peaks were too more narrow than in the test cavity, with the mechanical instability of the system, made impossible to create a stable error signal for the lock in of the laser. Also the bad coupling to the cavity mode plays a crucial role in the stability of the reflected signal.

4. Conclusions:

We studied the polarization readout noise of a signal coming from the output of a test cavity, and we characterized its Power Noise Spectral Density against optical power. We observed an enhancement of the technical noise of about 3 orders of magnitude, and we concluded the absence of a shot noise limited range. Main sources of technical noise arises in vibrations of the mirrors of the cavity, which in one hand, introduces fluctuations on the phase shifts induced to the resonating light, that leads to polarization fluctuations at the output of the cavity, and in the other hand, perturbs the geometry of the ray paths inside the cavity, leading to an unstable reflected and error signal for the lock in of the laser.

We haven´t observed an enhancement in our signal to noise ratio, by comparing the ratio between the calculated increment on the amount of signal, and the measured augmentation of noise, obtaining a decrement of SNR about 93%.

We have acquired quantitative knowledge about the different ways which mechanical instability of the system introduces noise to our measurement. We identified the bad quality of the lock as the main source of technical noise for the case of our test cavity, and we were not able to lock our laser in to the 1000 Finesse cavity due to the instability of the signal because of this vibrations.

We consider that looking for solutions to this mechanical instabilities, and improving the coupling to the cavity mode we can in principle obtain a better lock signal which hopefully leads to a less noisy cavity transmission.

References;

[1] Ian Daniel Leroux 2011 Squeezing collective atomic spins with an optical resonator (Massachusetts Institute of Technology).

[2] Monika Helene Schleier-Smith 2005 Cavity enabled spin squeezing for a quantum enhanced atomic clock (Harvard University)

[3] Marko Koschoreck 2010 Generation of Spin Squeezing in an ensemble of Rubidium 87 (Institute of Photonic Sciences and Universidad Politécnica de Cataluña)

[4] Marcin Kubasik 2009 Towards spin squeezing in atomic ensembles (Institute of Photonic Sciences and Universidad Politécnica de Cataluña)

[5] Vito Giovanni Lucivero 2014 Shot noise limited magnetometer with sub-pT sensitivity at room temperature *AIP Scitation.***6**.

[6] Naeimeh Behbood 2013 Real time vector-field tracking with a cold-atom magnetometer *Applied Physic Letters*